AECD - 2369

UNITED STATES ATOMIC ENERGY COMMISSION

NEUTRON-PROTON SCATTERING AT 90 MEV

by

Keith Brueckner
Walter Hartsough
Evans Hayward
Wilson M. Powell

University of California
Radiation Laboratory

This document is reproduced as a project report and is without editorial preparation. The manuscript has been submitted to The Physical Review for possible publication.

Date of Manuscript: September 10, 1948
Date Declassified: November 2, 1948

Issuance of this document does not constitute authority for declassification of classified copies of the same or similar content and title and by the same authors.

Technical Information Branch, Oak Ridge, Tennessee
AEC, Oak Ridge, Tenn., 5-16-49--850-A1468

PRINTED IN USA
PRICE 10 CENTS

NEUTRON-PROTON SCATTERING AT 90 MEV

By Keith Brueckner, Walter Hartsough, Evans Hayward, and Wilson M. Powell

ABSTRACT

An experimental measurement of the angular distribution of protons scattered by neutrons in the neutron beam of the 184-inch Berkeley cyclotron has been made with a Wilson cloud chamber with magnetic field. The results show that the scattering is not isotropic in the center of mass system and that it is not symmetric about 90 degrees. The peak of protons in the forward direction indicates that a certain amount of charge exchange is taking place between the neutron and proton.

* * * * *

The scattering of protons by neutrons of energies as high as 15 Mev has been studied by a number of observers.[1] Their results indicate that the scattering is isotropic in the center of mass system. Large changes in this distribution are to be expected when the de Broglie wavelength of the neutrons becomes smaller than the range of nuclear forces. In this experiment a hydrogen filled Wilson cloud chamber was placed in the neutron beam from the 184-inch cyclotron and the scattering angles of the knock-on protons determined. Simultaneously, Hadley et al[2] have been investigating this problem using counters. These two experiments together are expected to give an accurate determination of the angular distribution of protons scattered by neutrons of energies near 90 Mev, the cloud chamber giving assurance that no large systematic error is being made and the counter experiments giving the higher statistical accuracy for which they are a more suitable tool.

Deuterons accelerated by the 184-inch cyclotron reach a half-inch beryllium target with an energy of approximately 190 Mev. A large fraction of the high energy neutrons produced appear in a beam in the forward direction. The intensity of this beam drops to half value in approximately five degrees.[3] The energy distribution shows a maximum at 90 Mev. Both of these characteristics were predicted by Serber's stripping theory[4] for the deuteron and are particularly well adapted to the study of the scattering of protons by neutrons. The solid curve in Figure 1 gives the calculated energy distribution of the neutrons in the beam. This energy distribution was checked by a measurement of the energy spectrum of the protons leaving a thin target in the forward direction.[5] It has been assumed that the energy distribution is the same for both neutrons and protons. This beam was collimated as shown in Figure 2 so that it passed through the center of the Wilson cloud chamber in a beam 5/8 of an inch in diameter.

APPARATUS AND PROCEDURE

The cloud chamber (Figure 3) was of the rubber diaphragm type measuring 16 inches in diameter and 6 inches deep with a useful depth (i.e., illuminated region) of about 3-1/2 inches. The neutrons entered through a 5 mil aluminum window in the wall of the cylinder. It was filled with about 110 cm of hydrogen and saturated with an alcohol-water mixture, 70% alcohol by volume.

The magnetic field was supplied by a pair of Helmholtz coils which, when carrying a current of 4000 amperes, produce a field of 14,000 gauss. This field drops only 3% six inches from the center of the chamber. The power is supplied by a mine-sweeper generator, energized by a 150 hp motor; it is pulsed once every two minutes. It takes about 2 seconds for the current to rise to its maximum, where it remains steady for about .15 seconds before being turned off. During this interval of steady current the cloud chamber is expanded, and the cyclotron is pulsed near the end of the sensitive time of the chamber. Very sharp tracks are produced in this manner. Turbulence is minimized by maintaining the chamber at a constant temperature of 19.3°C. by means of a temperature controlled cir-

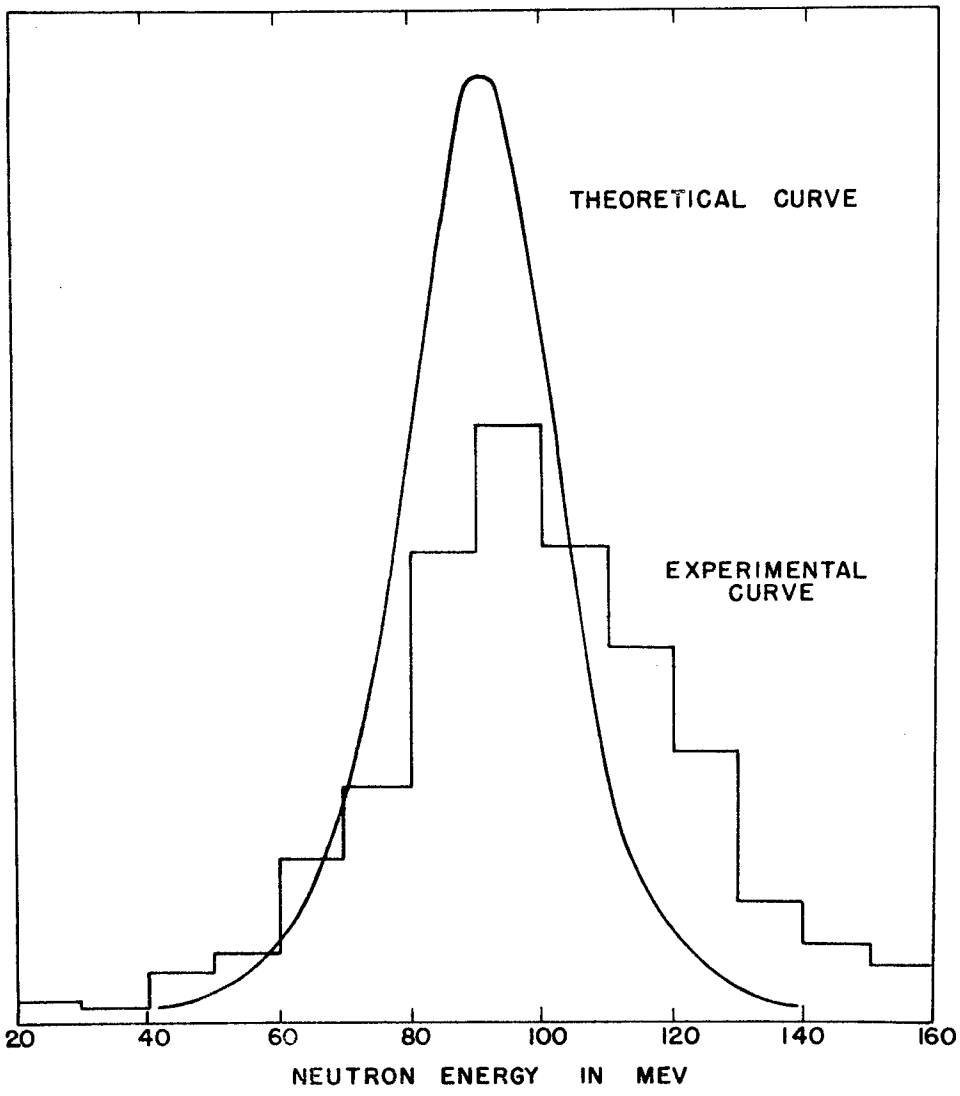

Figure 1. Theoretical and experimental energy distributions. The experimental histogram is based on the data compiled in Table 3 and corrected for the variation of the scattering cross section with energy.

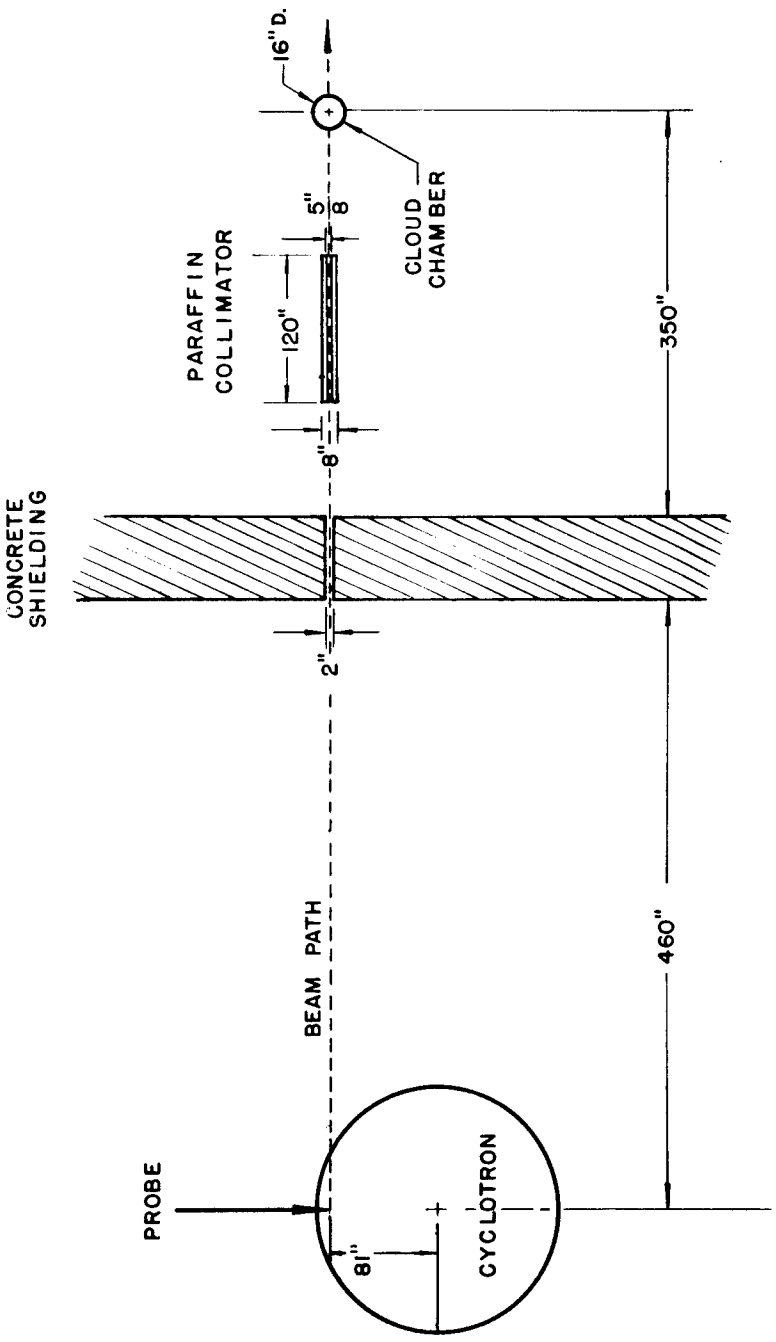

Figure 2. Experimental arrangement showing the positions of the cloud chamber and collimator relative to the cyclotron and shielding.

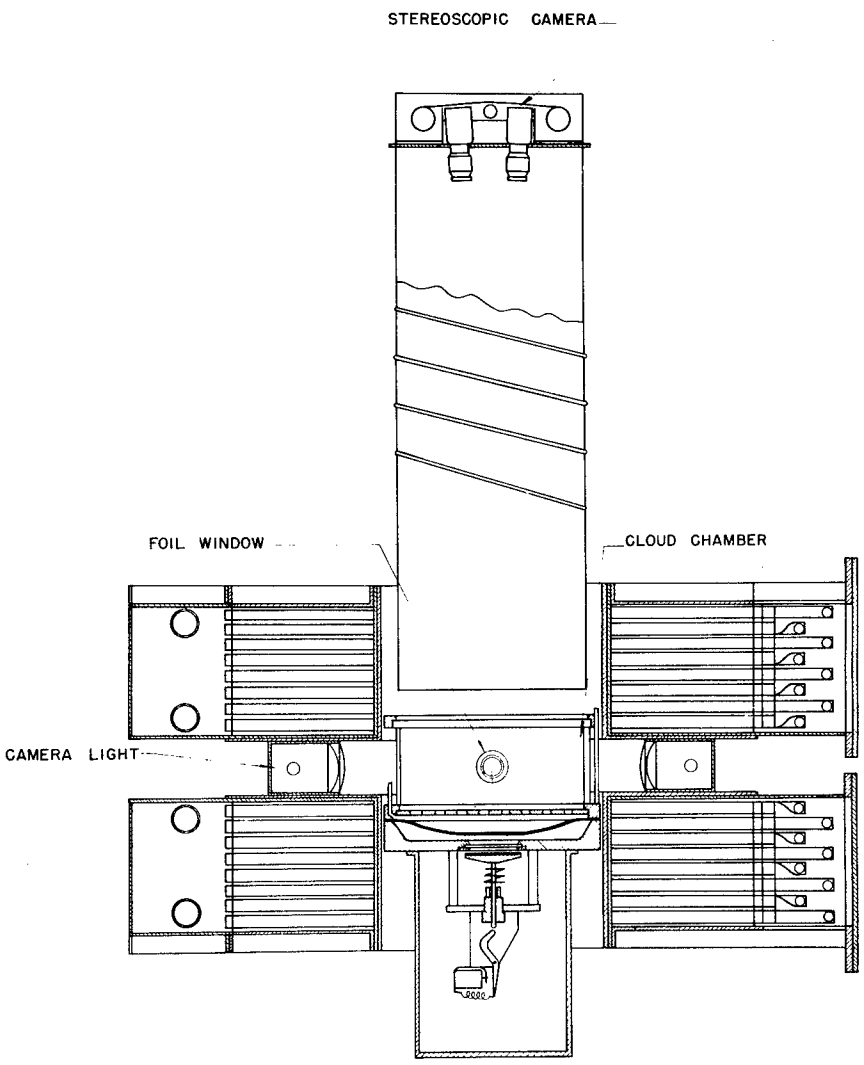

Figure 3. Schematic drawing of the cloud chamber and helmholtz coils.

culating water system. Two slow expansions were used between each fast expansion, the total time for a complete cycle being about 2 minutes. A clearing field of approximately 27 volts/cm was applied across the chamber and shorted out just before the expansion.

The illumination was obtained by discharging a pair of condenser banks of 256 μf each at 1700 volts through a pair of General Electric FT422 flash tubes. The flash tubes were mounted behind a pair of cylindrical lucite lenses to provide a parallel beam of light and were placed in the space between the Helmholtz coils so that the chamber was illuminated at right angles to the line along which it was photographed (Figure 3). The camera had no shutter, the length of the exposure being determined simply by the length of the flash, which was about 100 μsec. The photographs were taken at f16 with a stereocamera using a pair of Leica lenses of 127 mm focal length separated by 4.5 inches and about 52 inches from the black velvet on the bottom of the cloud chamber. The film was Eastman Super XX and cut in 100 foot strips 1.81 inches wide.

A 10-foot paraffin collimating tube (Figure 2) was placed between the concrete shielding of the cyclotron and the cloud chamber. This produced a neutron beam 5/8 inch in diameter at the cloud chamber. A transit at the far side of the cyclotron was used to line up the tube and the target with the cloud chamber. A very intense light source behind the eyepiece of the transit projected the cross-hair through the collimating system onto the chamber window assuring accurate alignment. Two lines were drawn on the top glass of the chamber accurately parallel to within half a degree with the neutron beam. These marks appeared on each photograph and were used to determine the zero reading for the beam angle, β.

REPROJECTION OF THE PHOTOGRAPHS

A double projector, Figure 4, with an optical system identical with that of the stereocamera threw a pair of life size images of the cloud chamber on a special coated glass (Eastman Recordak Green Translucent Screen, Type 75551). On the way to the screen the light passed through a piece of 3/4-inch plate glass in order to correct for the distortions introduced by the 3/4-inch top glass of the cloud chamber.

The procedure used in making the measurements involves first the adjustment of the film so that it is in the same relative position it had when the picture was taken. This was done by placing the green screen horizontal and at the proper height so that the distance between it and the projector lenses was 52 inches. Its position then corresponded to the bottom of the cloud chamber. Two wire crosses, sewn to the bottom of the chamber exactly eleven inches apart, served as fiducial marks. The projector lenses were closed down to f8 and their focus adjusted so that the space between the fiducial marks was eleven inches for each projected image. Then the two images were brought into register by means of three fine screw adjustments on the film holder behind one of the projection lenses.

In order to obtain sufficiently brilliant projected images it was necessary to use the Western Union concentrated arc lamp type 100. This made it possible to close down the projector lenses so that the reproduction was exact.

The reprojected track (Figure 4) is superimposed on the measuring plate with the beginning of the track normal to the horizontal axis of rotation of the plate AA. The beam angle, β, is measured in the horizontal plane between the direction of the neutron beam and the horizontal projection of the tangent BB to the beginning of the track. The dip angle, α, in the vertical plane is measured to the tangent BB. The curvature is measured by matching it to one of a series of concentric arcs ruled on a lucite template. A single line on the lucite template perpendicular to all the arcs is simultaneously matched to the line AA to insure the accurate measurement of the angles α and β. The scatter angle, $\theta = \cos^{-1} \cos \alpha \cos \beta$ can then be calculated and the energy E_n of the incident neutron can be obtained from the measured radius of curvature, ρ_S, of the knock-on proton. Neglecting a small relativistic correction, the energy E_p of the proton is given by the expression

$$E_p = \frac{e^2}{2\,mc^2} \left(\frac{H\rho_H}{\cos \alpha} \right)^2$$

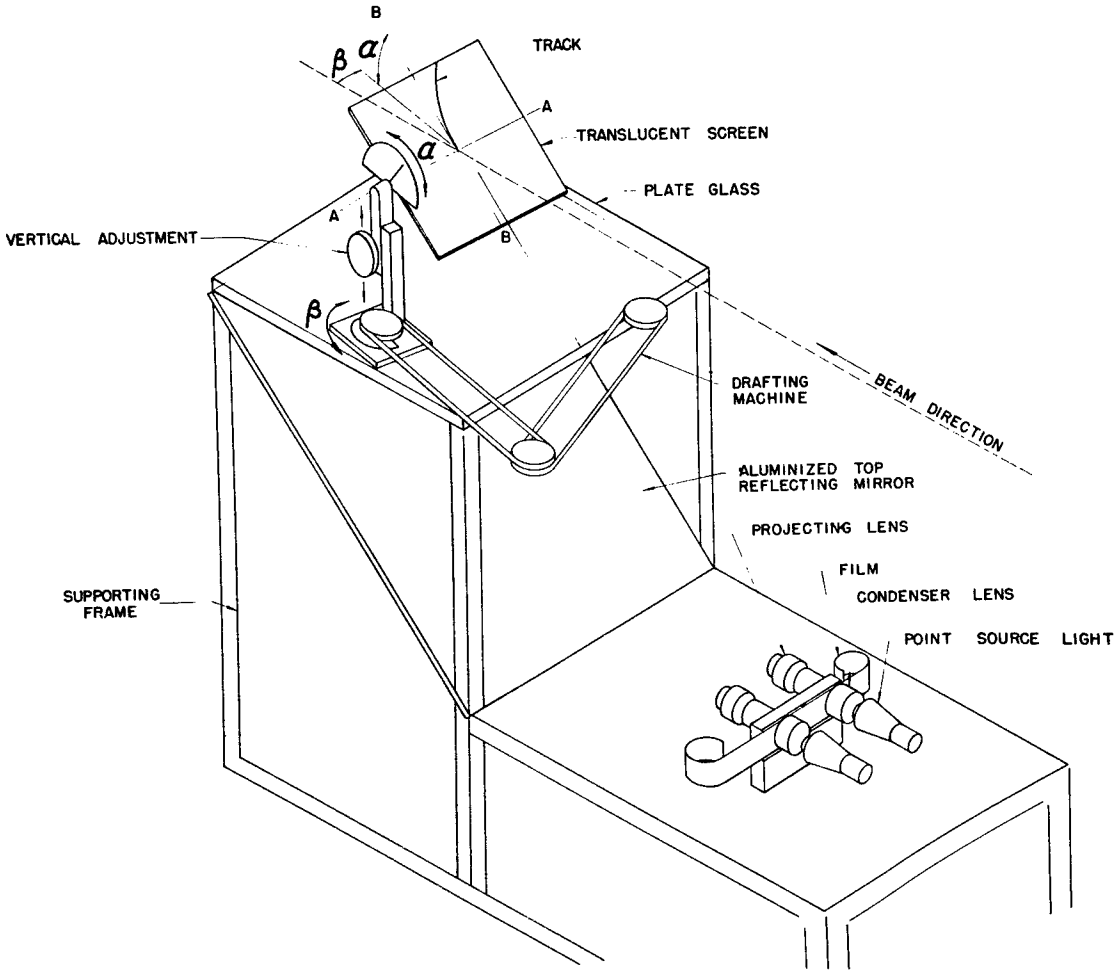

Figure 4. Schematic drawing of the reprojection apparatus.

$$E_n = \frac{e^2}{2\,mc^2}\left(\frac{H\rho_H}{\cos^2\alpha}\right)^2 \frac{1}{\cos^2\beta}$$

where ρ_H is the curvature of the track if it is measured in the horizontal plane. It is related to the curvature, ρ_S, which is actually measured, by the expression $\rho_H^2 = \rho_S^2 \cos^4\alpha$.

Since the aim of the experiment is to measure the angular distribution of the protons scattered by neutrons of energies near 90 Mev, it was necessary to exclude events caused by lower energy neutrons. Hadley et al set a lower limit for the neutron energies of 65 Mev. An examination of the experimentally determined energy distribution in Figure 1 shows a minimum at 40 Mev. The number of neutrons between 40 Mev and 65 Mev is sufficiently small so as not to invalidate a comparison between the two experiments. For these reasons a lower limit of 40 Mev was chosen and higher energies determined merely as a check on the experimental accuracy as described herein.

It was also necessary to set an upper limit to the scatter angle that would be included, since the particles scattered at large angles have short ranges and might be overlooked. Eighty-four degrees was chosen as the largest angle to be accepted in the data, because the range of the knock-on proton scattered at 85 degrees by a 40 Mev neutron would be 0.8 cm. A track of this length would still have been observable but a slightly shorter one would not.

Many auxiliary experiments have been performed as checks on the data. These are listed herewith.

1) The accuracy of these measurements depends on the assumption that all the neutrons producing events went through the chamber in the same direction. The validity of this assumption was checked by the observation that the ratio of the number of knock-on protons appearing outside the collimated beam to that in the beam was approximately one in a hundred. The volume occupied by the beam is small compared to the total illuminated volume of the chamber so we may conclude that the number of knock-on protons produced by uncollimated neutrons is negligible.

2) The accuracy of the projecting apparatus was checked by taking pictures of a drafting triangle at various positions in the chamber and then measuring the angles by reprojection. The reprojected angles were found to be correct to within 1/2 degree for small dip angles and to within 1 degree for a dip angle of 60 degrees.

3) The question of whether high energy tracks were being missed because of their low ionization has been investigated. Since protons with energies of about 100 Mev knocked out of the glass were clearly visible, it has been assumed that none of those starting in the gas have been missed. As an additional check an auxiliary camera was placed so that it viewed the cloud chamber at an angle such that each track scattered more light into it. No tracks were found in the pictures taken with the auxiliary camera that were not also clearly visible in the photographs taken with the stereocamera, although the tracks appeared to be considerably blacker.

4) It was also suggested that some nuclear disintegrations might be confused with knock-on protons. Such an event might consist of a proton track associated with a very short recoil nucleus. A set of pictures, taken with a cloud chamber filled with He and O_2 contained many stars due to the disintegration of O_2 but only two scattered protons. This number was commensurate with the number to be expected from the hydrogen in the vapor.

5) The data were thoroughly checked for turbulence since this is one of the most important sources of error. Every fifth expansion was made without the magnetic field and with a block of paraffin in front of the chamber window so that there would be an ample number of protons in these pictures (Figure 9a). If the tracks curved more than 1 mm in 20 cm, the pictures were excluded, and never fewer than 40 pictures in a turbulent strip were discarded in order to be certain that there was no turbulence in the pictures taken when the magnetic field was on. Also certain parts of the cloud chamber near the edges were found to be turbulent; therefore, tracks that started near the entrance and exit windows were omitted. The region of the cloud chamber from which tracks would be accepted was decided upon before the tracks were measured. This region was a cylinder with a diameter of about 1 inch and having a length of about 12 inches.

6) The data were selected and measured by two people independently. About one out of every 40 tracks was overlooked by one of the two observers; therefore, the chance that both would miss the same one is very small. Their measurements were reproducible to less than 1 degree in dip angle and

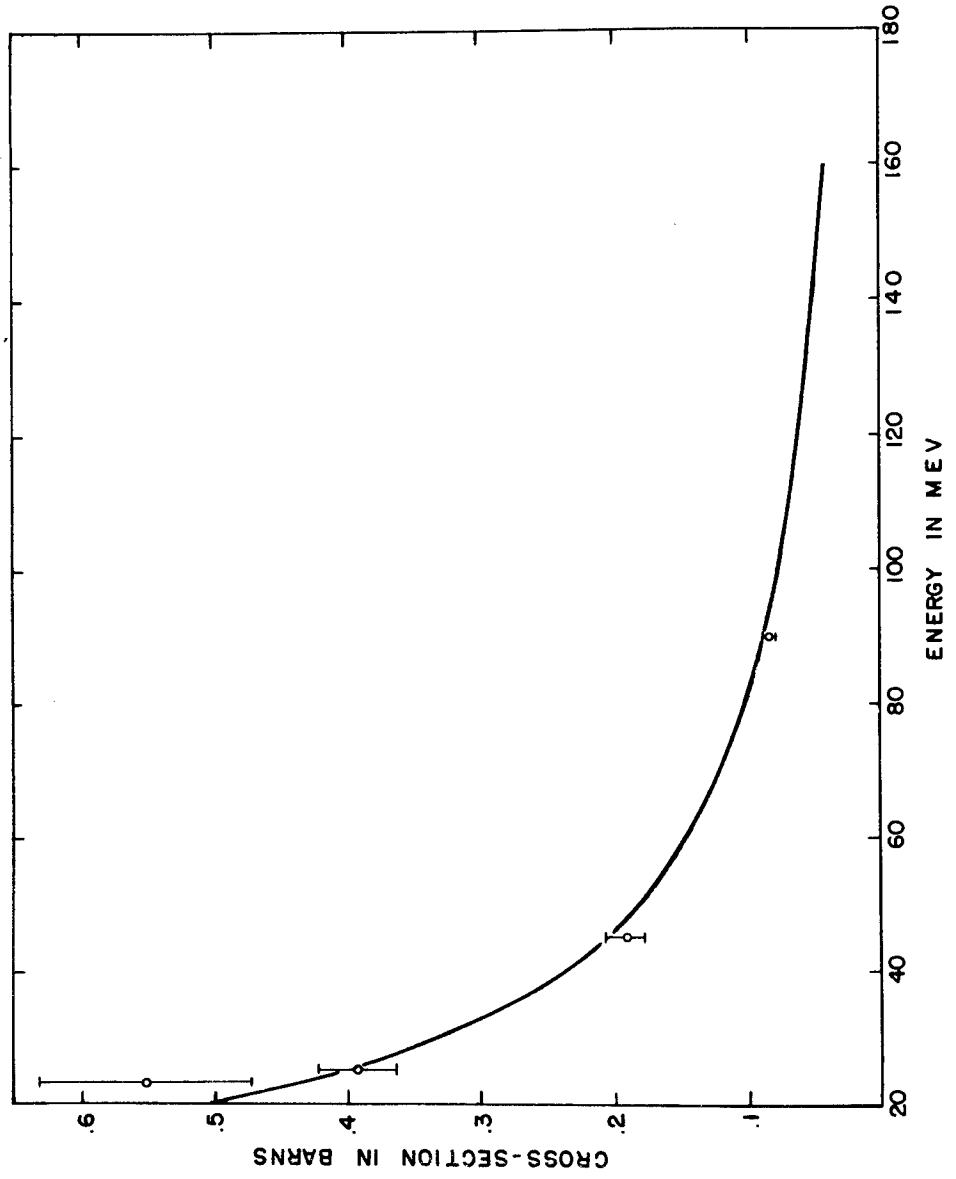

Figure 5. Energy dependence of the scattering cross-section used to obtain the energy distribution of the neutrons.

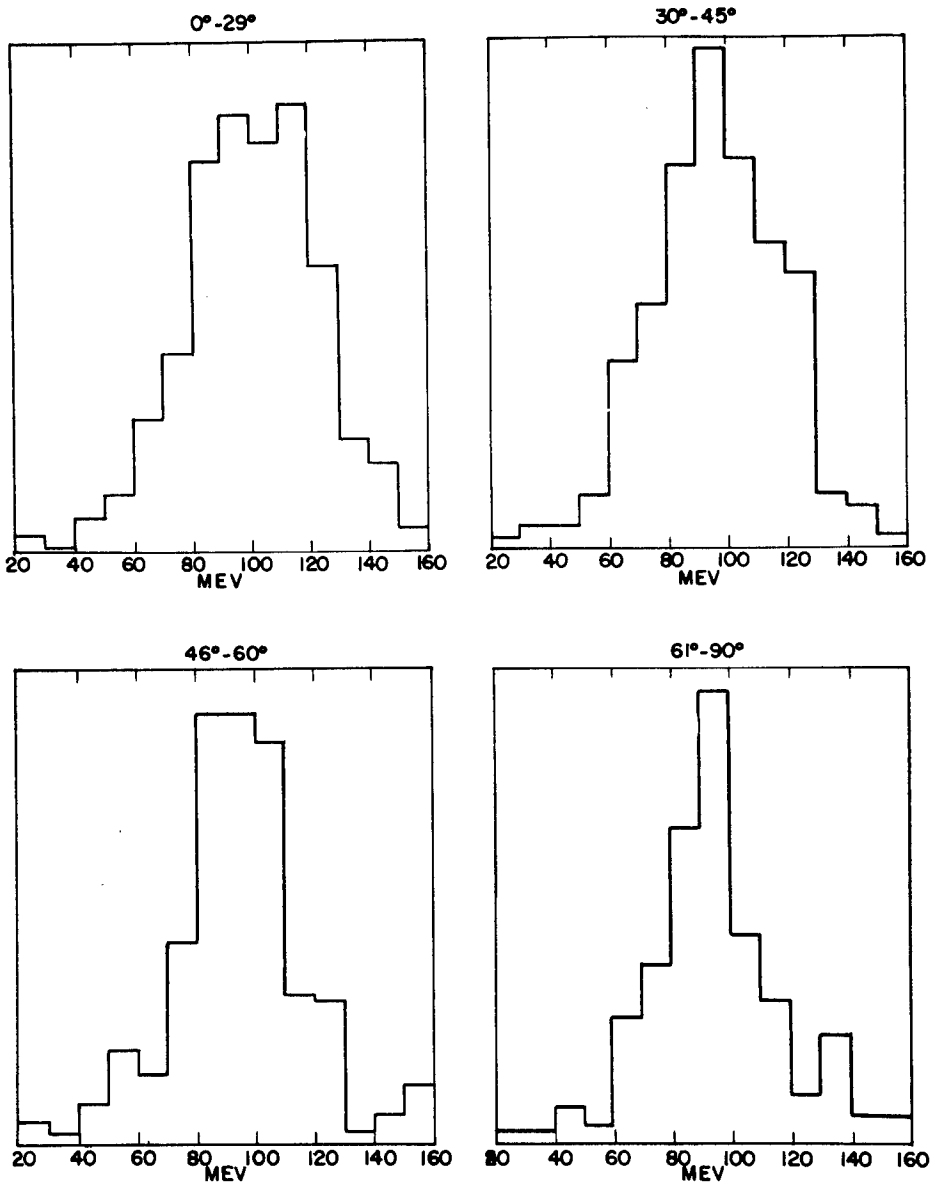

Figure 6. Energy distribution for the angular intervals θ = 0-29, 30-45, 46-60, and 61-90 degrees, respectively.

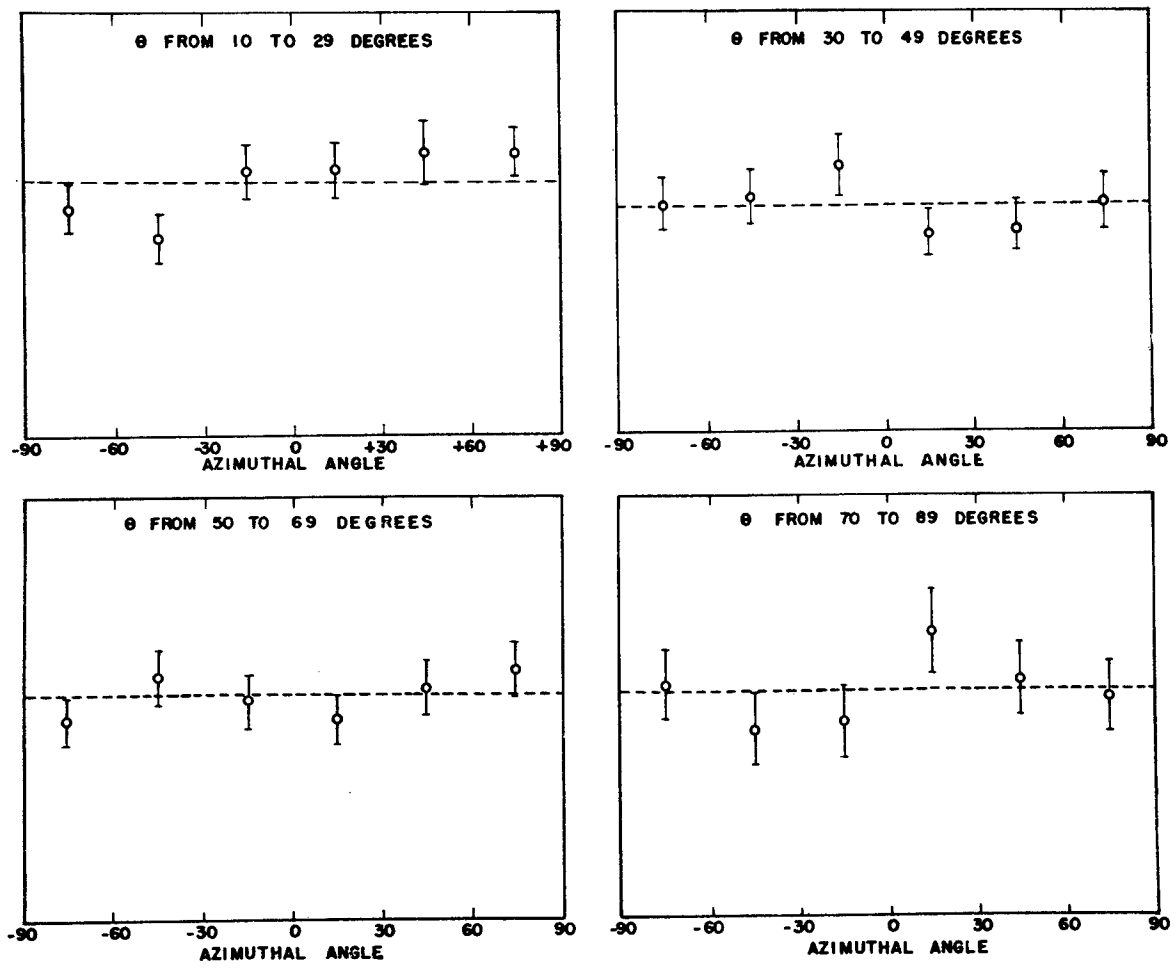

Figure 7. Azimuthal distributions for four scattering angle intervals. The dotted lines represent the mean.

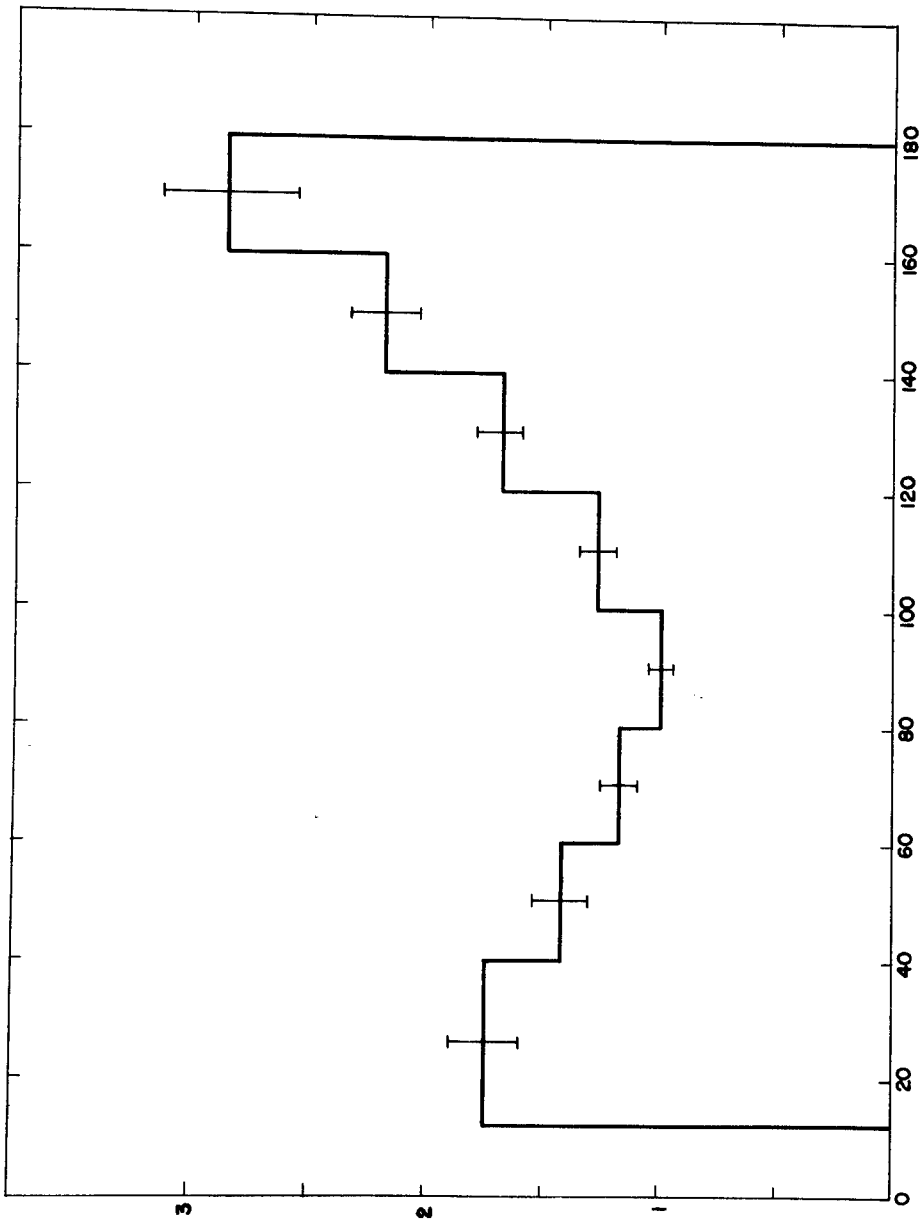

Figure 8. Number of neutrons scattered per unit solid angle in the center of mass system. The standard deviations are based only on the number of tracks. Only those recoils due to neutrons with energies greater than 40 Mev have been included.

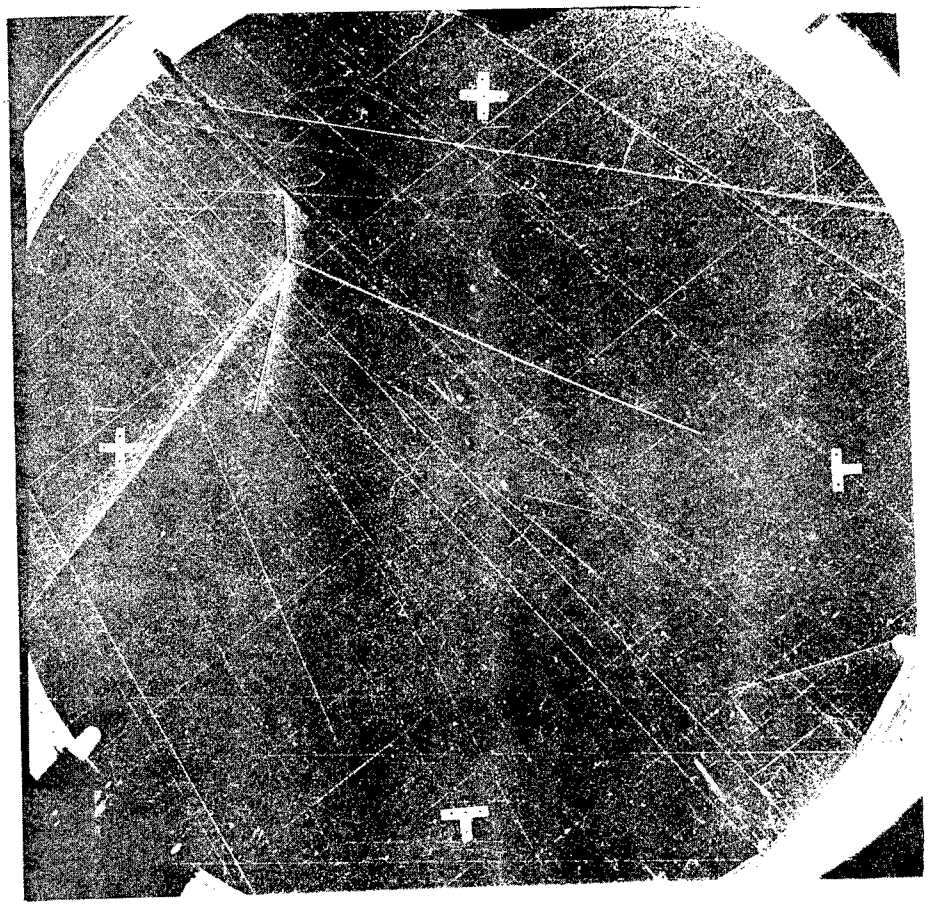

Figure 9a. Photograph taken without the magnetic field and with a block of paraffin in front of the chamber window. The straight parallel lines are the clearing field wires. The direction of the neutron beam is from the upper right-hand corner to the lower left.

Table 1. Comparison of angular distribution for two sets of data.

Neutron Scatter Angle	Cameras at 0 degrees 871 tracks		Cameras at 45 degrees 893 tracks	
	Number observed	S. D.	Number observed*	S. D.
12 - 40	93	9	100	10
40 - 60	105	10	117	11
60 - 80	113	11	112	11
80 - 100	105	10	109	11
100 - 120	127	11	126	11
120 - 140	133	12	143	12
140 - 160	128	11	109	11
160 - 180	57	8	54	7

*multiplied by $\frac{871}{893}$

1/2 degree in beam angle. If the discrepancy was larger, the track was remeasured twice, independently, and satisfactory agreement was always reached.

7) The data, which consist of 1764 knock-on protons, were taken in two sets; the first yielding 871 and the second, 893 protons. During the first set the two lenses of the camera straddled the direction of the beam, while for the second set the camera was rotated through 45 degrees. This should have revealed the presence of any large systematic errors in the measurements. Turning the camera through 45 degrees also increases the stereoscopic effect for those tracks scattered at large angles to the beam direction and thus makes the measurement of them more accurate. The angular distributions of the scattered protons in the two sets (Table 1) were not found to differ significantly. These distributions include only protons scattered by neutrons having energies greater than 40 Mev. The energy distributions based on 812 tracks (those with $\alpha > 50$ degrees excluded) of the first set and on 246 of the second set were found to be in good agreement so that the energies for the remaining protons were not measured except to distinguish recoils from neutrons with energies above and below 40 Mev.

8) Another check was made by comparing the estimated probable error in the energy with that obtained from the half-width of the experimental energy distribution. An approximate expression for the fractional error in the neutron energy may be obtained by differentiating the foregoing expression for the neutron energy:

$$\frac{\Delta E}{E} = .67 \left[\left(\frac{2\Delta H}{H}\right)^2 + \left(\frac{2\Delta\rho H}{\rho H}\right)^2 + (4 \tan\alpha\Delta\alpha)^2 + (2 \tan\beta\Delta\beta)^2\right]^{1/2}$$

$\frac{\Delta H}{H}$ is about $\pm$ 3% due to the radial variation of the field and to small errors in reading the ammeter. The fractional error in the radius of curvature, $\frac{\Delta\rho}{\rho}$, arises first from the error in measurement, $\pm$ 5%, and secondly from the "curvature" produced in the track by turbulence in the cloud chamber. This second error is given by $\frac{\rho H}{\rho_T}$ where ρ_T is the radius of curvature due to turbulence. This term depends on the energy and is most important for high energy tracks. In calculating the probable error ρ_T has been assumed to be 800 cm. The second term in the preceding expression may then be written:

$$\left[2(.05)\right]^2 + \left[\frac{2\rho}{800}\cos\beta\right]^2$$

Table 2.

		α					
		0°	20°	40°	60°	70°	80°
β	0°	15.4	14.3	12.7	17.7	32.6	65
	20°	14.8	13.8	12.2	17.7	31.8	65
	40°	13	12.3	11.5	17.6	32	64
	60°	10.9	10.6	10.9	17.7	32	64
	70°	10.5	10.5	11.3	18.2	32	64
	80°	13.7	13.8	14.7	20.5	34	65
	85°	23.4	23.6	24.2	28.1	38.7	67

The estimate of the error in the dip angle, α, is based on the reproducibility of the measurements:

$$\pm 1\text{-}1/2^\circ \quad 0 < \alpha < 50^\circ$$
$$\pm 2^\circ \quad \alpha = 60^\circ$$
$$\pm 2\text{-}1/2^\circ \quad \alpha > 60^\circ$$

The error in the beam angle, β, is $\pm$ 1 degree; this includes the error in marking the beam direction on the top of the chamber as well as the error in measurement. The results obtained by substituting these estimates in the foregoing formula are given in Table 2 for a 60 Mev neutron. The theoretical energy distribution of the neutrons is given in Figure 1. The energies of the primary neutrons were experimentally obtained from the scatter angle and the curvature of about 1000 recoil protons. This energy distribution, if corrected for the variation of cross section with energy, gives the distribution in energy of the incident neutrons as shown in Table 3. In order to compare the experimental energy distribution of the neutrons with the theoretical one it is necessary to assume a cross section which varies with the energy of the neutrons. Figure 5 is a curve fitted to the experimental points of Sleator[6] at 23 Mev, Sherr[7] at 25 Mev, Segrè[8] at 45 Mev, and Cook, McMillan, and Sewell[9] at 90 Mev and extrapolated beyond 90 Mev by Christian[10]. This curve shows a cross section varying as 1/E and is the one used for the purposes of this comparison. The histogram in Figure 1 gives the experimentally determined energy distribution of neutrons after correction for the variation of energy with cross section. Only neutrons producing recoil protons with dip angles less than 50 degrees are included because of the large error in the determination of their energies. In comparing theory and experiment it has been assumed that the actual distribution of the neutrons is that given by the theory. Since the spread in the experimental curve is due first to the spread in the theoretical distribution and secondly to experimental errors, the probable error in the energy measurements may be obtained by comparing the half-widths of the two curves. We obtain $\pm$ 13%. Selecting the angular group for which the energy measurements should be the best ($30^\circ < \beta < 65^\circ$ and $0 < \alpha < 25^\circ$) (Figure 5), we obtain a probable error of $\pm$ 10%. These probable errors compare very favorably with those given in Table 2 so we conclude that no large systematic errors are being made.

8) If we assume that the angular distribution of the scattered protons does not depend critically on the neutron energy, we can check the accuracy of the measurements by comparing the experimental energy distributions at various scatter angles. Four such distributions are given in Figure 6, again with dip angles greater than 50 degrees excluded. They show only the expected spread in energy.

9) Finally, the azimuthal distribution (Figure 7) indicates that no significant number of tracks has been missed or measured incorrectly. It should be emphasized that the errors in measurement of the incident neutron energy are large compared to the errors in the measurements of the scatter angle. The experimental angular distribution is, therefore, more reliable than the energy spectrum.

Table 3.

Mev	Number of tracks	Energy distribution σ(barns)	$N/\sigma \times 10^{-2}$
20 - 30	37	.40	0.9
30 - 40	20	.28	0.7
40 - 50	42	.20	2.1
50 - 60	49	.16	3.1
60 - 70	92	.130	7.1
70 - 80	118	.112	10.5
80 - 90	194	.093	20.9
90 - 100	217	.081	26.8
100 - 110	153	.072	21.2
110 - 120	110	.066	16.7
120 - 130	72	.060	12.0
130 - 140	29	.054	5.4
140 - 150	17	.049	3.5
150 - 160	12	.046	2.6

RESULT

The angular distribution has been measured for those protons corresponding to neutrons with energies exceeding 40 Mev and includes those protons scattered in the angular interval 0 to 84 degrees in the laboratory system. Those particles scattered beyond 85 degrees have such a short range that they might be overlooked; to be certain that none were missed, all those scattered beyond 84 degrees have been excluded. 40 Mev has been chosen as the neutron energy below which tracks would not be accepted because there are so few neutrons in the energy interval 35 to 45 Mev. Not more than 5 tracks could have been incorrectly included in or excluded from the data. The data, determining the angular distribution, are compiled in Table 4. The histogram in Figure 8 shows the number of neutrons scattered per unit solid angle in the center of mass system. A small relativistic correction has been neglected which would move the experimental points only by a small fraction of their standard deviations. The number per unit solid angle in the center of mass system is:

$$\frac{dN}{d\omega} = \frac{dN}{2\pi \operatorname{Sin} \theta \, d\theta}$$

where θ is the scatter angle in the laboratory system. The data have been divided into eight groups; the first seven groups each include 20 degrees and the last, 28 degrees. The relative number of protons scattered per unit solid angle has been obtained by dividing the number of particles in each group by the average value of the sine for the interval. The standard deviations (Table 4) are based only on the number of tracks. The experimental errors, which amount to 2 degrees at the most, increase the standard deviations by not more than 25% for all the points except the one corresponding to 160 to 180 degrees. Here the process of averaging the sin 2θ gives only a fair approximation because the variation of the sine is not linear over the interval. The amount of error introduced cannot be ascertained from the data; however, it is estimated to increase the indicated error by not more than 50 per cent.

Table 4.

Neutron scatter angle	Number observed I*	Number observed II†	Number observed I × geometrical correction	Cos interval	Intensity in arbitrary units I*	Intensity in arbitrary units II†
12 - 40	126	196	217	.205	1.74 ± .15	1.58 ± .11
40 - 60	145	225	227	.262	1.43 ± .12	1.42 ± .09
60 - 80	187	228	235	.324	1.20 ± .08	1.16 ± .08
80 - 100	227			.374	1.00 ± .06	
100 - 120	256			.329	1.28 ± .08	
120 - 140	280			.270	1.71 ± .10	
140 - 160	240			.179	2.21 ± .14	
160 - 180	112			.064	2.88 ± .27	

*I – includes only proton tracks with dip angles less than 51 degrees.
†II – includes tracks of all dip angles.
Errors are standard deviations based on the number of tracks

Those tracks that dip up or down from the horizontal by more than 50 degrees have been excluded because it is difficult to measure them accurately enough to be certain that they are due to neutrons with energies greater than 40 Mev. We have corrected for this omission by multiplying by a suitable geometrical factor based only on the assumption that the scattering is azimuthally symmetrical:

$$f = 1 - \frac{\pi}{2\cos^{-1}\left(\frac{\sin 50^\circ}{\sin\theta}\right)}$$

Those points we obtain with the actual number of tracks scattered with dip angles greater than 50 degrees are given in Table 5. Although those points lie slightly below those obtained using the geometrical weighting factor, they agree well within the probable errors.

We conclude first that the scattering is not isotropic in the center of mass system; furthermore the details of the distribution indicate that it is not symmetrical about 90 degrees. Secondly, the peak protons in the forward direction indicates that a certain amount of charge exchange is taking place between the neutron and proton. This work is in good agreement with that done by Hadley et al[2] covering the neutron scatter angles from 65 to 180 degrees.

ACKNOWLEDGMENTS

The authors wish to express their appreciation to Professor Ernest O. Lawrence for his interest in this work. Professor Emilio G. Segrè and Professor Robert Serber have made many valuable suggestions. Marguerite Hayward and Raymond E. Butler gave much essential technical assistance, John Swensson and Wallace Kilpatrick made many of the measurements. Paul Hernandez was responsible for the mechanical design of the major part of the equipment. Melvin E. Chun was in charge of the electrical equipment.

Table 5.

θ	$N(\alpha > 50)$	N_t	$N(\alpha > 50)f$
0 - 2	11		
3 - 4	24		
5 - 6	14		
7 - 8	26		
9 - 10	37		
11 - 12	44		
13 - 14	48		
15 - 16	58		
17 - 18	51		
19 - 20	39		
21 - 22	60		
23 - 24	52		
25 - 26	59		
27 - 28	50		
29 - 30	59		
31 - 32	53		
33 - 34	52		
35 - 36	35		
37 - 38	50		
39 - 40	66		
41 - 42	23		
43 - 44	49		
45 - 46	61		
47 - 48	41		
49 - 50	53		
51 - 52	45	53	52
53 - 54	42	44	52
55 - 56	19	40	37
57 - 58	35	45	48
59 - 60	32	46	46
61 - 62	30	42	45
63 - 64	39	53	60
65 - 66	31	49	48
67 - 68	27	49	44
69 - 70	18	32	30
71 - 72	33	47	54
73 - 74	28	42	47
75 - 76	21	34	36
77 - 78	11	24	19
79 - 80	11	17	19
81 - 82	11	17	20
83 - 84	11	15	20

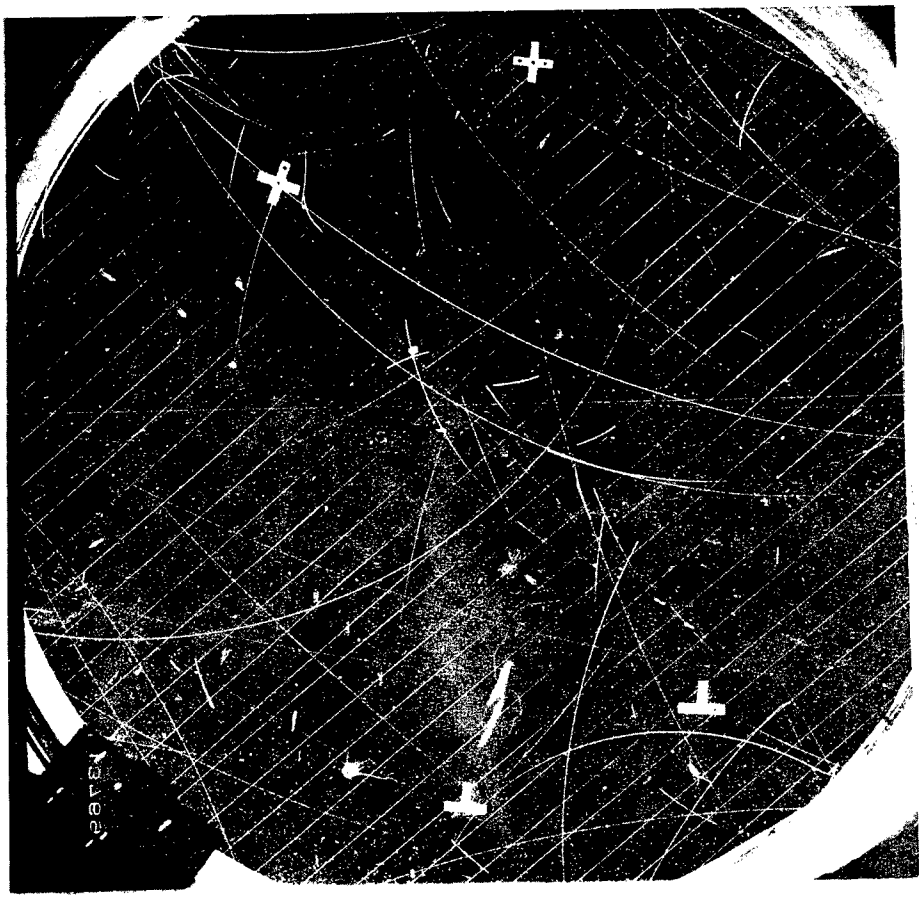

Figure 9b. Photograph taken without the magnetic field and with a block of paraffin in front of the chamber window, showing several examples of knock-on protons. The straight parallel lines are the clearing field wires. The direction of the neutron beam is from the upper right-hand corner to the lower left.

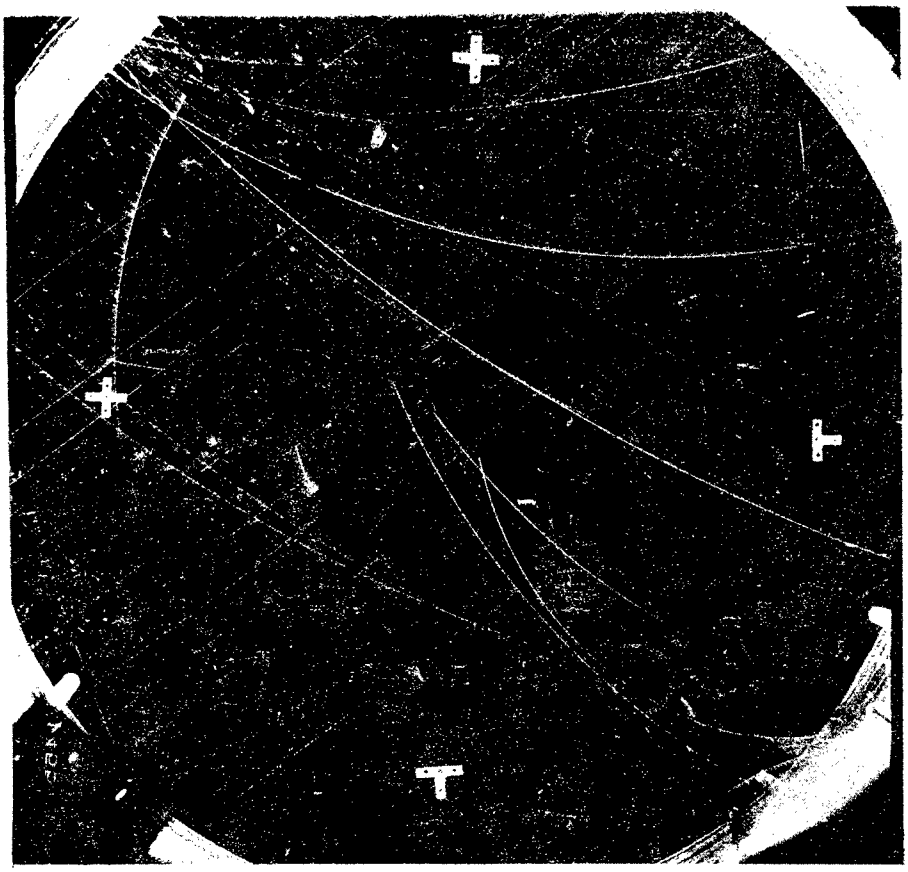

Figure 9c. Photograph taken without the magnetic field and with a block of paraffin in front of the chamber window, showing several examples of knock-on protons. The straight parallel lines are the clearing field wires. The direction of the neutron beam is from the upper right-hand corner to the lower left.

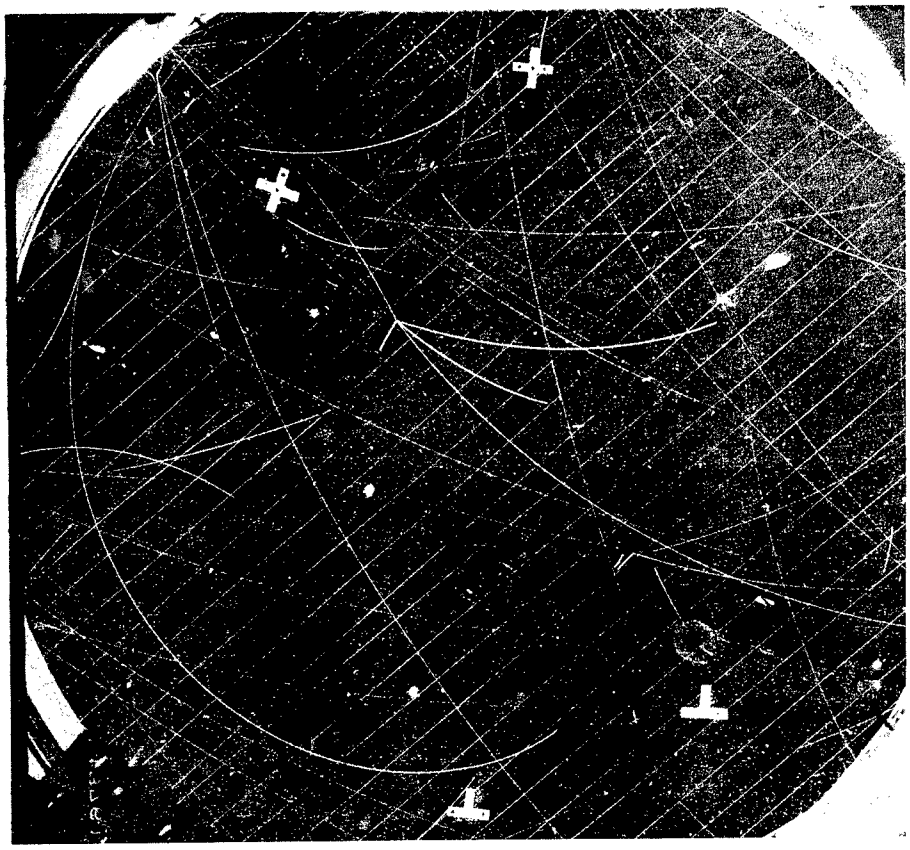

Figure 9d. Photograph taken without the magnetic field and with a block of paraffin in front of the chamber window, showing a nuclear disintegration. The straight parallel lines are the clearing field wires. The direction of the neutron beam is from the upper right-hand corner to the lower left.

REFERENCES

1. Kruger, P. G., W. E. Shoupp, and F. W. Stallman, Phys. Rev. 52:678 (1937).
   Bonner, T. W., Phys. Rev. 52:685 (1937).
   Dee, P. I. and C. W. Gilbert, Proc. Roy. Soc. 163:265 (1937).
   Champion, F. C., and C. F. Powell, Proc. Roy. Soc. 183:64 (1944).
   Laughlin, J. S., and P. G. Kruger, Phys. Rev. 73:197 (1947).
2. Hadley, J., E. L. Kelly, C. E. Leith, E. Segré, C. Wiegand, and H. F. York, Phys. Rev. 73:1114 (1948).
3. Helmholz, A. C., E. M. McMillan, D. C. Sewell, Phys. Rev. 72:1003 (1947).
4. Serber, R., Phys. Rev. 72:1007 (1947).
5. Chupp, W. W., E. Gardner, T. B. Taylor, Phys. Rev. 73:742 (1948).
6. Sleator, W., Phys. Rev. 72:207 (1947).
7. Sherr, R., Phys. Rev. 68:240 (19).
8. Segré, E., Private communication.
9. Cook, L., E. M. McMillan, and D. Sewell, Phys. Rev. 72:1264 (1947).
10. Christian, R., Private communication.

END OF DOCUMENT